

Temporal hotspots of rabbit abundance

1 Models of spatiotemporal variation in rabbit abundance reveal management 2 hotspots for an invasive species

3 Stuart C Brown^{1*}, Konstans Wells², Emilie Roy-Dufresne¹, Susan Campbell³, Brian Cooke⁴,
4 Tarnya Cox⁵, Damien A. Fordham¹

5 ¹ The Environment Institute and School of Biological Sciences, University of Adelaide,
6 Adelaide, South Australia 5005, Australia

7 ² Department of Biosciences, Swansea University, Swansea SA2 8PP, UK

8 ³ Biosecurity and Regulation, Primary Industries and Regional Development, Albany,
9 Western Australia 6330, Australia

10 ⁴ Institute for Applied Ecology, University of Canberra, Canberra, ACT 2601, Australia

11 ⁵ Vertebrate Pest Research Unit, NSW Department of Primary Industries, Orange, New South
12 Wales 2800, Australia

13 * Corresponding author. Email: s.brown@adelaide.edu.au

Stuart C Brown: s.brown@adelaide.edu.au; Konstans Wells: k.l.wells@swansea.ac.uk;
Emilie Roy-Dufresne: emilie.roy-dufresne@adelaide.edu.au; Susan Campbell:
susan.campbell@agric.wa.gov.au; Brian Cooke: brian.cooke@canberra.edu.au; Tarnya Cox:
tarnya.cox@dpi.nsw.gov.au; Damien A. Fordham: damien.fordham@adelaide.edu.au

14 **Abstract:**

15 The European rabbit (*Oryctolagus cuniculus*) is a notorious economic and environmental pest
16 species in its invasive range. To better understand the population and range dynamics of this
17 species, 41 years of abundance data have been collected from 116 unique sites across a broad
18 range of climatic and environmental conditions in Australia. We analyzed this time series of
19 abundance data to determine whether inter-annual variation in climatic conditions can be
20 used to map historic, contemporary, and potential future fluctuations in rabbit abundance
21 from regional to continental scales. We constructed a hierarchical Bayesian regression model
22 of relative abundance that corrected for observation error and seasonal biases. The corrected
23 abundances were regressed against environmental and disease variables in order to project
24 high spatiotemporal resolution, continent-wide rabbit abundances. We show that rabbit
25 abundance in Australia is highly variable in space and time, being driven primarily by inter-
26 annual variation in temperature and precipitation in concert with the prevalence of a non-
27 pathogenic virus. Moreover, we show that inter-annual variation in local spatial abundances
28 can be mapped effectively at a continental scale using highly resolved spatiotemporal
29 predictors, allowing “hotspots” of persistently high rabbit abundance to be identified.
30 Importantly, cross-validated model performance was fair to excellent within and across
31 distinct climate zones. Long-term monitoring data for invasive species can be used to map
32 fine-scale spatiotemporal fluctuations in abundance patterns when accurately accounting for
33 inherent sampling biases. Our analysis provides ecologists and pest managers with a clearer
34 understanding of the determinants of rabbit abundance in Australia, offering an important
35 new approach for predicting spatial abundance patterns of invasive species at the near-term
36 temporal scales that are directly relevant to resource management.

37 **Keywords:**

38 climate drivers, invasion hotspot, invasive species management, long-term monitoring, N-
39 mixture model, *Oryctolagus*, random forests

40 **Introduction:**

41 Long-term datasets are vitally important for the successful management of native and
42 invasive species (Yoccoz et al. 2001). In a macro-ecological context, such datasets should
43 ideally report the abundance of the species through time at multiple sites, capturing a broad
44 range of niche requirements (Magurran et al. 2010). These types of spatiotemporal explicit
45 datasets, whilst being rare (Whittaker et al. 2005), can help to identify climatic,
46 environmental and biotic processes that determine species range limits and drive the structure
47 and dynamics of geographic ranges (Caughley et al. 1988, Gaston 2003). Furthermore, they
48 can be used to predict spatiotemporal variation in population fluctuations which is crucial for
49 effective conservation (Channell and Lomolino 2000) and pest and invasive species
50 management (Strayer et al. 2006).

51 Differences in duration, methodology, frequency of sampling, spatial grain and spatial
52 extent within and between studies, makes systematic comparisons of inferences of long-term
53 population trends, from multiple studies problematic (Magurran et al. 2010, Pagel et al.
54 2014). Notwithstanding these difficulties, the integration of long-term spatially explicit
55 datasets from disparate sources, with varying spatial and temporal scales, is becoming more
56 common in macroecological studies as a means of forecasting patterns of spatial abundance
57 in time and space (Mellin et al. 2012), and to better understand ecological impacts of invasive
58 species (Strayer et al. 2006). The development of statistical approaches that allow sampling
59 and temporal biases (that result in false variation; Martin et al. 2005), among other sources of
60 uncertainty in abundance time series data (e.g., imperfect detection; Joseph et al. 2009), to be
61 identified and explicitly modelled, is facilitating better estimates of spatiotemporal variation
62 in local-to-regional species abundance patterns (Magurran 2007, Joseph et al. 2009, Schurr et
63 al. 2012).

64 Although abundance data are still typically analyzed using the average or maximum
65 count per unit transect (Buckland et al. 2015), N-mixture models (models with a mixed
66 binomial-Poisson likelihood), which estimate relative abundance based on replicated counts
67 (Royle 2004), are being used with increasing frequency to explicitly account for detection
68 probability in spatially explicit estimates of abundance (Aubry et al. 2012, Guillera-Arroita
69 2017), including invasive species (Wells et al. 2016b). Such models essentially produce a
70 bias-corrected abundance estimate, that can then be used to examine trends in population
71 fluctuations and abundances. To do this, corrected abundance data are combined with
72 environmental and climatic information, and where available, data on biotic interactions (i.e.
73 covariate effects; Royle 2004), to determine potential drivers of abundances. These statistical
74 relationships can then be used to make projections of abundance, providing opportunities to
75 assess population trends and geographic range limits across space and time (Joseph et al.
76 2009, Schurr et al. 2012).

77 The abundances and subsequent ecological impacts of invasive species are
78 exceedingly variable through time in their invasive range (Sofaer et al. 2018), making them
79 highly suited for N-mixture modelling approaches (Joseph et al. 2009, Guillera-Arroita
80 2017). For example, the occupancy and abundance rates of invasive species can change over
81 short time scales as a result of shifting evolutionary pressures (Phillips et al. 2006, Cox
82 2013), modifications in community composition (Mutze et al. 2016), and changes in species
83 interactions (Lurgi et al. 2018). This temporal variability means that invasive species are
84 typically not in equilibrium with their environment (Elith et al. 2010). Therefore, the
85 collection of long-term count data at spatiotemporal resolutions that allow for acute and
86 chronic effects of abiotic and biotic conditions on abundance to be teased apart using robust
87 statistical approaches is vital for generating estimates of population variation for invasive
88 species. These estimates will lead to better ecological and economic outcomes if the
89 mechanisms that affect population fluctuations of invasive species can be identified and
90 managed accordingly (Strayer et al. 2006).

91 Abundance, not probability of occurrence, is the currency of invasive species
92 management. This is because ecological mechanisms of range limits and shifts can be better

93 understood using abundance data (Fordham et al. 2012) and spatiotemporal estimates of
94 abundance and subsequent variability are frequently used to maximize the efficacy of on-the-
95 ground management efforts to control invasive species (Simberloff 2003). For example,
96 efforts for managing rabbits in their invasive range are often reduced when population size is
97 perceived to be relatively low, allowing resources to be prioritized elsewhere (Wells et al.
98 2016a). Moreover, time series abundance estimates are important for the development of
99 spatially explicit and dynamic population models for invasive species management (Mellin et
100 al. 2016), enabling management intervention strategies to be directly tested (Fordham et al.
101 2013a). This is because time series abundance estimates enable key demographic rates to be
102 estimated, including finite rates of population growth (Hone 1999), and for models to be
103 calibrated (Cabral and Schurr 2010). Therefore, modelling spatiotemporal abundance patterns
104 of invasive species provides resource managers with some distinct advantages over modelling
105 occurrence.

106 The European rabbit (*Oryctolagus cuniculus*) is an invasive pest species in several
107 regions around the world (Cooke 2012); but is a threatened species in its native range on the
108 Iberian peninsula, where it is a multifunctional keystone species that engineers habitat and
109 provides prey to consumers (Delibes-Mateos et al. 2008, Fordham et al. 2013b). In Australia,
110 *O. cuniculus* occurs across > 70 % of the mainland (Stodart and Parer 1988) and is well
111 adapted to the broad range of climatic conditions of the central and southern parts of the
112 continent (Cooke et al. 2018a), making it one of Australia's most abundant invasive
113 vertebrate species (Cooke 2012). It negatively effects Australia's unique biodiversity directly
114 through outcompeting native species for food and shelter (Cooke 2012), altering vegetation
115 composition (Mutze et al. 2016), and, indirectly, by maintaining invasive predator
116 populations (Lurgi et al. 2018). Furthermore, rabbits adversely affect the agro-economy with
117 an attributed economic loss of approximately A\$200m annually (Cooke et al. 2013).

118 Recently, more than 50 years of historical and contemporary rabbit abundance survey
119 data, from across the invasive range of rabbits in Australia, were combined with high
120 resolution weather, climate and environmental information to create the Australian National
121 Rabbit Database (Roy-Dufresne et al. 2019a). This dataset provides new and important

122 opportunities to better manage rabbits in Australia through a stronger understanding of their
123 population fluctuations and range dynamics. To date, there has been no Australia-wide
124 assessment of spatiotemporal rabbit abundances and fluctuations. Such an assessment is
125 needed to identify where, and under which environmental conditions rabbits attain high and
126 stable abundances, due to population recruitment and resistance to population perturbations.
127 Using this information in predictive models to generate high spatiotemporal resolution maps
128 of rabbit abundance will enable more targeted rabbit management at local-to-regional scales,
129 enabling the control of invasive rabbits to potentially be better optimized (Fordham et al.
130 2012, Lurgi et al. 2016). This is because invasive species management decisions are
131 typically based on populations in specific habitats and locales, involving time-horizons of
132 seasons to decades (Rout and Walshe 2013, Wells et al. 2016a).

133 Here we combine spotlight count data from 116 sites collected over 41 years (1972 –
134 2012 inclusive) for mainland Australia for *O. cuniculus* (Roy-Dufresne et al. 2019a). Our
135 focal period starts approximately 20 years after the introduction of myxomatosis – a highly
136 infectious and often fatal rabbit disease caused by the myxoma virus – to mainland Australia
137 in 1950. The focal period cover the introduction of Rabbit Hemorrhagic Disease Virus
138 (RHDV) in 1995 (Pech and Hood 1998) and its establishment in rabbit populations. We apply
139 a multi-level hierarchical N-mixture model to these data to “correct” for important biases
140 (namely detection error and bias due to seasonal reproduction and abundance fluctuations) in
141 annual estimates of abundance; and then use machine learning algorithms to determine the
142 relative influence of climate, environment and disease on spatiotemporal variation in rabbit
143 abundance in Australia. Our two-step approach provides a computationally efficient method
144 for generating range-wide, high-resolution spatially (~5 km) and temporally (annual) explicit
145 projections of abundance for a well-established invasive species, which can then be used to
146 reveal hotspots of abundance and to elucidate the drivers of the structure and dynamics of
147 their geographic ranges. Such information is needed to effectively management invasive
148 species at local-to-regional scales through targeted control measures (Baker and Bode 2016,
149 Lurgi et al. 2016).

150 **Methods:**

151 The key steps used to analyze time series count data for rabbits and predict spatiotemporal
152 ‘hotspots’ of abundance are shown schematically in Figure 1.

153 *Spotlight data:*

154 The spotlight data collated in the Australian National Rabbit Database covers the broad range
155 of climatic and environmental conditions that rabbits inhabit in Australia (Figure 2). These
156 data were collated from several different sources, mostly regional researchers affiliated with
157 state-level governmental institutions. We only consider data records with complete
158 information regarding: (1) geolocation; (2) survey dates; (3) transect length (limited to
159 plausible values ≥ 1 and ≤ 100 km); and (4) rabbit encounters (0 counts were included). This
160 resulted in 116 unique grid-cell sites (result of aggregating all count data into 5 km² grid cell
161 units) which we subsequently used to model rabbit abundances in space and time.

162 *Climate and environmental data*

163 The aggregated site data was matched to gridded 5 km² data containing information on total
164 daily precipitation (mm), and minimum and maximum temperature (°C) data from the TERN
165 e-MAST facility (<http://portal.tern.org.au>). These climatic variables have been shown to
166 influence the burrow emergence behavior of rabbits, and therefore affect detection probability
167 of rabbits during spotlight surveys (Ballinger and Morgan 2002). Furthermore, grid-cell
168 information on the location and length of the transect, annual climatic conditions (e.g.
169 previous summer total precipitation, previous winter average minimum temperature),
170 environmental conditions (e.g. proportion of agricultural land within the 5km² grid cell,
171 proportion of clay soils), and disease proxies (e.g. prevalence of non-pathogenic rabbit
172 calicivirus [RCV-A1]; Liu et al. 2014) was also joined to the aggregated data.

173 Full details of the climatic and environmental variables used in our analysis are
174 provided in Appendix S1: Table S1.

175 *Climate zone*

176 To account for regional differences in seasonal rabbit population growth and recruitment
177 (Poole 1960, Hone 1999, Mutze et al. 2002, Wells et al. 2016b), the spotlight records were

178 grouped into climate zones, where long-term climatic conditions were similar. No
179 geophysical properties (e.g. elevation) were included in the stratification units as they are not
180 expected to significantly influence rabbit distributions and abundance in Australia (Cooke
181 1977, Fordham et al. 2012, Wells et al. 2016b, Roy-Dufresne et al. 2019b). The climate zones
182 were identified by first doing a principal component analysis on 12 climatic variables (e.g.
183 30-year mean maximum temperature, precipitation seasonality), and then an iterative test to
184 identify the number of “climate zones” required to adequately describe the diversity of
185 climatic conditions. Using a k-means clustering algorithm (R Core Team 2017), the iterative
186 test involved minimizing the within-cluster sum of squared errors (SSE) for a range of
187 potential cluster solutions (2 – 12 clusters) and identifying the point of inflection where the
188 SSE levelled off. Since rabbit reproduction and regional population fluctuations are often
189 highly seasonal (Mutze et al. 2002, Wells et al. 2016b), the spotlight abundance data was
190 grouped by climatic zones where long-term average climate and resource availability (Noble
191 1977) is assumed to be similar (Figure 2). In doing so, we assume that all rabbit populations
192 from a climate zone follow similar seasonal population fluctuations through synchronous
193 timing of reproduction. Climate zones ranged from warm, humid summer conditions in the
194 north with austral summer (DJF) dominated rainfall (Zone 8) to mild summers and cool
195 winters, with winter dominated rainfall conditions in the south (Zone 5). A full description of
196 the climate zones is provided in Appendix S1: Table S2, with mean (\pm S.D) for each variable.
197 The climate zones are available in Data S1: Brown_et_al_RabbitAnalysisOutputs.nc.

198 *Correcting abundance count data:*

199 We established a generalized multi-level hierarchical mixture model in a Bayesian
200 framework to derive an index of standardized relative yearly rabbit abundance free of well-
201 established and important sampling biases that is comparable across surveys. Specifically, we
202 used an N -mixture model (Royle 2004) to model spotlight counts $c(t,k)$ for each of the
203 repeated surveys k during a given year in for cell r at time step t as:

$$204 \quad c(t,k) \sim \text{Bin}[N_r(t), p(t,k)] \text{ and } N_r(t) \sim \text{Pois}[\Lambda(r,t)] \quad (1)$$

205 where, we assumed each count to be a random draw based on the underlying true but
 206 unknown abundance $N_r(t)$, governed by the Poisson density $\Lambda(r,t)$.

207 We modelled the detection probability $p(t,k)$ with a *logit*-link function as:

$$208 \quad \text{logit}[p(t,k)] = \mu(r) + \eta(c) + v_1(ds) + v_2(t_{max}) + v_3(t_{min}) + v_4(pr_{day}) \quad (2)$$

209 where, $\mu(s)$ accounts for variation in detection probability between cells (r), $\eta(c)$ accounts for
 210 variation between climate zones (c), $v(ds)$, $v(t_{max})$, $v(t_{min})$, and $v(pr_{day})$ allow for variation
 211 between different data sources (corresponding to different survey teams), and daily weather
 212 variables. Note that $\Lambda(r,t)$ represents the relative local abundance at the time of observation
 213 and is not corrected for transect length nor seasonal bias in counts.

214 The spotlight surveys were conducted in different seasons and along transects of
 215 different lengths, therefore, the estimate of detection probability needs to account for
 216 spatiotemporal variability in recruitment (Wells et al. 2016b) and survey efforts (Ballinger
 217 and Morgan 2002, Barrio et al. 2009). Doing so will reduce potentially important sources of
 218 bias in estimates (Link et al. 2018). We used random regression models, following Wilson et
 219 al. (2005), to account for potentially important variation due to seasonal bias and different
 220 transect lengths. For this, we modelled $\Lambda(r,t)$ on a log-scale (natural logarithm):

$$221 \quad \ln[\Lambda(r,t)] = \omega(r,y,m) + \ln[transL(i)] \quad (3)$$

222 where, $\omega(r,y,m)$ is the intercept of the random regression model, which can vary across
 223 cells (r), years (y), and months (m); and $transL(i)$ is the corresponding length of the transect
 224 in km for the respective sample.

225 We modelled $\omega(r,y,m)$ further based on a two-level mean/hyperprior models with
 226 Gaussian error of the general form $\mathcal{N}[H, \sigma^2]$ with mean H and variance σ^2 in order to derive
 227 an estimate of the most likely yearly abundance independent of the seasonal bias in counts:

$$228 \quad \omega(r,y,m) \sim \mathcal{N}[H_{RY,\omega}(r,y), \sigma_{R,\omega}(r)^2] \quad (4)$$

229 and

$$230 \quad H_{RY,\omega}(r,y) \sim \mathcal{N}[H_{R,\omega}(r), \sigma_{R,\omega}(r)^2] \quad (5)$$

231 where, $H_{RY,\omega}(r,y)$ denotes the population-level annual ‘average’ density distribution for each
 232 site and year, while the respective variance $\sigma_{R,\omega}(r)^2$ is a random estimate of the inter-
 233 seasonal variance in population fluctuations for each cell (r) according to the variation in

234 monthly counts from different sites. $H_{R,\omega}(r)$ denotes the site-level ‘average’ relative
235 abundance and $\sigma_{R,\omega}(r)^2$ interannual variance in population fluctuations.

236 Our model was fitted in a Bayesian framework using Markov Chain Monte Carlo
237 (MCMC) sampling in the software JAGS 4.3.0, operated via the R software (v 3.5.1; R Core
238 Team 2017) with the ‘rjags’ package (Plummer 2016). Priors were specified as $\sigma \sim \text{Gamma}$
239 $(0.01, 0.01)$ and $H_{R,\omega}(r) \sim \mathcal{N}(0, 10)$.

240 We applied posterior predictive model diagnostics to assess whether the model
241 assumptions were good approximations of the data generating process. Bayesian P -values
242 ~ 0.5 indicate a good model fit whereas values close to 0 or 1 indicate an increasing
243 discrepancy between model predictions and observation data (Gelman et al. 1996). We
244 calculated 5000 values as posterior distributions for all parameters of interest after mixing
245 and convergence of two parallel MCMC chains was confirmed visually and with the Gelman-
246 Rubin diagnostic (most values < 1.2) after a burn-in of 50,000 MCMC samples.

247 *Modelling rabbit abundances in space and time:*

248 Modelled corrected abundances ($H_{RY,\omega}(r, y)$; Appendix S1: Figure S1) – extracted from the
249 Bayesian model as the mode of the posterior density distributions – were aligned with the key
250 predictor variables in Appendix S1: Table S1. To generate predictions of rabbit density we
251 opted to use a readily available and straight forward machine learning approach, random
252 forests (RF; Breiman 2001), implemented in the ‘randomForest’ package for R (Liaw and
253 Wiener 2018). This decision was made because compared to most Bayesian methods, RFs
254 enable a broad range of model selection and cross-validation procedures that are not
255 commonly used in an MCMC context due to practical computing time issues (Kéry and
256 Schaub 2011). Essentially, we use the hierarchical model for correcting abundances for
257 various sources of bias, while we use RFs for exploring and accounting for any non-linear
258 patterns between corrected abundances and climate and environmental correlates in spatial
259 predictions.

260 For simplicity, we categorized the annual model corrected abundance estimates into
261 ‘low density’ (corresponding to ≤ 45 rabbits/km², assuming an effective transect width of 0.1

262 km) and ‘high density’ (corresponding to > 45 rabbits/km²). These values were chosen as
263 there was a natural break in the calculated density values, and it has been demonstrated that at
264 densities < 50 rabbits/km², damage to perennial native vegetation is minimized across both
265 temperate and arid environments (Mutze et al. 2016). This binary variable allowed us to use a
266 two-step regression model (Mellin et al. 2012) to predict rabbit abundance through time and
267 space (Figure 1). To do this we used a binary classification variable (high/low density) as a
268 predictor in our regression model in order to make spatiotemporal explicit predictions of
269 rabbit abundance. Thus, the model generates spatial estimates of abundance conditional on
270 whether density in a given cell is high or low.

271 A binary classification RF model was first created using the aforementioned density
272 classes. Due to the unbalanced nature of the classes *a posteriori* tuning of the probability
273 threshold for classification (default = 0.50) was performed to maximize model accuracy.
274 Using this approach, once the classification RF model had been trained (using the default
275 threshold), a series of thresholds between 0 and 1 were tested to maximize the area under the
276 ROC curve (Kuhn 2018). A separate regression RF model was then built which incorporated
277 the RF predicted density classes as an additional correlate for predicting rabbit abundance.
278 The two-step procedure necessitated the use of RF predicted rabbit density for cell r at time
279 $t-1$.

280 To train and assess the performance of our RF models, we used 1,000 repeats of a
281 Monte-Carlo cross-validation procedure, whereby the data was randomly split (without
282 replacement) into 80/20 training/test splits. Models consisting of 2001 trees were built on the
283 80% splits and tested on the 20% holdout test samples. The cross-validation was carried out
284 using the ‘caret’ package for R (Kuhn 2018). Correlations between the environmental and
285 climatic correlates (Appendix S1: Table S1) were tested, and with a few exceptions, were not
286 strongly positive or negatively correlated (Appendix S1: Figure S2). As random forests are
287 able to deal with correlated variables (Breiman 2001), we did not perform any feature
288 selection or reduction on the correlates included in the model. Variable importance was
289 calculated using an unscaled permutation-based method (Liaw and Wiener 2018). Spatial
290 autocorrelation in the residuals of predicted RF abundance was conducted using Moran’s I

291 statistic using an inverse distance relationship with a threshold of 1130 km (the average
292 pairwise distance between all sampling points).

293 Spatially and temporally explicit estimates of rabbit density and abundance (i.e.
294 maps), were then predicted for Australia between 1972 and 2012. Hotspots of high rabbit
295 abundance were identified for each year that abundance predictions were made by
296 approximating a cumulative relative frequency distribution (CRFD) curve as a function of
297 relative rabbit abundance plotted against the relative frequency distribution of abundance for
298 a given year (Bartolino et al. 2011a). The count data for the CRFD curve was pooled across
299 all sites within each year. Unlike traditional hotspot identification methods which require a
300 user-defined threshold (Bartolino et al. 2011a, b, Cayuela et al. 2011), the CRFD method
301 identifies the hotspot threshold as a function of the CRFD curve. The method involves
302 calculating the slope of the tangents to the CRFD curve, with the hotspot threshold being
303 identified as the value where the slope of the tangent is 45° (Bartolino et al. 2011a). Using the
304 thresholds for each year, the predicted abundance maps were then converted to a series of
305 binary hotspot maps. The proportion of time spent in “hotspot” conditions across the study
306 period was then determined for each cell by counting the number of times a cell was
307 classified as a hotspot, divided by the number of years.

308 *Climate envelope and confidence mask*

309 To constrain predictions of corrected density and abundance to climate conditions used to
310 train the model and, in doing so, avoid model extrapolation, we identified all cells for
311 Australia that fell within the extremes (i.e. highest and lowest) of the climatic variables that
312 were used to define the climate zones. In doing so we constrain our predictions of density and
313 abundance to cells that fall within the bounds of our long-term climatic variables and limit
314 extrapolation to “unseen” climatic conditions (Liu et al. 2014). All maps in Data S1:
315 `Brown_et_al_RabbitAnalysisOutputs.nc` are clipped to this climate envelope.

316 To identify regions of “low confidence,” we did a PCA using the top 10
317 environmental and climatic variables that were considered important for both the
318 classification and regression RF models, and using the first 3-components as pseudo-3-

319 dimensional-coordinates, we identified individual grid cells in 3-dimensional space that were
320 outside a 3-dimensional convex-hull of the sampling sites within each of the climate zones.
321 That is, 3-dimensional polygons were constructed, with vertices defined by the pseudo-3-
322 dimensional-coordinates of all cells for which we had samples within each climate zone. Any
323 additional cells (i.e. grid cells where no monitoring had occurred) that exist inside the 3-
324 dimensional boundary of this polygon can be considered inside the “environmental space” of
325 the study sites within each climate zone. Cells outside this 3-dimensional polygon, have
326 climatic or environmental conditions not seen at the sites used within the climate zone. This
327 process allowed us to identify grid-cells where our predictions of corrected density and
328 abundance were outside the environmental and climatic space of all monitoring sites in the
329 study, essentially creating a mask of low confidence where predictions were likely to have
330 been extrapolated in environmental and/or climatic space, rather than interpolated. The
331 confidence mask is supplied in Data S1: Brown_et_al_RabbitAnalysisOutputs.nc.

332 **Results:**

333 *Drivers of detection*

334 Coefficient estimates for the drivers of detection varied in magnitude and sign across climate
335 zones (Table 1). Within 5 of the 9 climate zones (1, 2, 4, 6, and 7) an increase in maximum
336 daily temperature decreased the probability of detection (mean = -0.23, S.D. = 0.11), whilst
337 for the remaining 4 zones (3, 5, 8, and 9) it resulted in an increase in detection probability
338 (mean = 0.28, S.D. = 0.18). Increases in minimum daily temperature (except for climate zone
339 4) and daily total precipitation, resulted in slight increases in detection probability (minimum
340 daily temperature: mean = 0.04, S.D. = 0.03; precipitation: mean = 0.05, S.D. = 0.02).

341 Gelman-Rubin diagnostics for hyperpriors indicated good convergence of the
342 detectability model: (i) maximum daily temperature = 1.08 (upper CI = 1.32); (ii) minimum
343 daily temperature = 1.17 (upper CI = 1.59); (iii) daily precipitation = 1.09 (upper CI = 1.31).

344 *Determinants of spatiotemporal patterns of density and abundance*

345 The five most important predictor variables, as calculated using permutation importance, for
346 the classification RF model of rabbit density (high/low) were: temperature seasonality,

347 proportion of irrigated agriculture within the grid-cell, two-year lagged average temperature,
348 distance to permanent water, and the prevalence of the benign RCV-A1 calicivirus (Appendix
349 S1: Figure S3). Evaluation of these variables with Accumulated Local Effects (ALE; Apley
350 2016) plots (Appendix S1: Figure S4) suggests that at sites with lower temperature
351 seasonality and lower mean annual temperatures in the years ($n = 2$) prior to the survey, there
352 was an increased probability of high rabbit densities. Furthermore, at the few sites that were
353 sampled on irrigated land, sites with as little as $\sim 7.5\%$ irrigated agriculture within a 5km grid-
354 cell were 60% more likely to have high rabbit densities than a conditional averaged site
355 (Appendix S1: Figure S4). The probability of a site having high density decreased with
356 distance from permanent water until $\gtrsim 20\text{km}$. Although some sites that had high densities
357 were situated very far away from permanent water sources ($> 150\text{km}$; Appendix S1: Figure
358 S4). As benign RCV-A1 prevalence increased above $\sim 20\%$ the probability of a site having
359 high abundance was $\sim 25\%$ greater than the average site (Appendix S1: Figure S4). Taken
360 together the results from the classification RF model suggest that at sites with stable, cool
361 temperatures, with abundant pastures (owing to irrigation, and proximity to permanent water
362 sources), and prevalent RCV-A1, rabbit densities will be higher. Cross-validated performance
363 of the classification model was excellent across climate zones and in most cases fair to
364 excellent within climate zones (Table 2). The mode of the predicted rabbit densities and the
365 mean prediction probability confidence (1972 – 2012) is shown in Figure 3. The complete
366 time series of density maps is shown in Data S1: Brown_et_al_RabbitAnalysisOutputs.nc.

367 The five most important variables influencing model predictions of rabbit abundance
368 (excluding rabbit density class from the previous year; Appendix S1: Figure S3) were:
369 precipitation the year prior, average winter minimum temperature the year prior, two-year
370 lagged total precipitation, precipitation seasonality, and the prevalence of benign RCV-A1.
371 These variables exhibited similar importance within the regression RF model (Appendix S1:
372 Figure S3). ALE plots of the regression model (Figure 4) suggest that at sites where one-year
373 lagged precipitation was $\gtrsim 400\text{mm}$ the year prior, and one-year lagged minimum winter
374 temperatures $\gtrsim 4^\circ$, there was an increase in rabbit abundance. As for the classification model,
375 examination of two year lagged average temperature suggests that at sites with lower mean

376 annual temperatures ($\lesssim 16^\circ \text{C}$) rabbit abundances are higher. Like with the classification RF,
377 this suggests that in cool, wet areas rabbit abundances will be higher. However, for the
378 regression RF the effects of precipitation are likely acting as a proxy for pasture availability.
379 In contrast to the classification model, the plot of the association between abundance and the
380 prevalence of benign RCV-A1 suggests that as virus prevalence increases, abundances will
381 decrease (Figure 4). Regression model performance was excellent across climate zones and in
382 most cases fair to excellent within climate zones (Table 1). With some exceptions, the 95%
383 prediction intervals of the regression RF model were able to capture the variability in the
384 corrected abundance counts (Figure 5). Moran's I suggested no residual spatial
385 autocorrelation ($I = 0.002$, $z = 0.166$, $p = 0.87$). The mean of the predicted rabbit abundances
386 and the mean standard deviation of the abundances through time (1973 – 2012) are shown in
387 Figure 3. All abundance maps are available in Data S1:

388 [Brown_et_al_RabbitAnalysisOutputs.nc](#).

389 *Variable interactions*

390 Examination of second-order interactions for the regression model (Figure 4b) suggest that
391 for sites with $> 20\%$ prevalence of benign RCV-A1 and with mean annual temperatures
392 below $\sim 16^\circ \text{C}$, the combined effects are positive on abundance. Conversely, second-order
393 interactions between precipitation and RCV-A1 (Figure 4c) suggest that at sites with $\lesssim 20\%$
394 prevalence, and annual precipitation is $> 600\text{mm/year}$, there is a net positive effect on rabbit
395 abundance suggesting increased precipitation, and therefore an increase in potential pasture
396 availability, could lead to higher abundances at sites where there is low immunity to lethal
397 RHDV. Furthermore, after the main effects of the variables (namely precipitation and RCV-
398 A1 prevalence) have been accounted for, there is a negligible effect of RCV-A1 prevalence
399 on rabbit abundance in areas of high rainfall ($> 600\text{mm/year}$) as illustrated by the relative
400 “flatness” and values of the interaction surface (Figure 4c).

401 *Hotspots of abundance*

402 Predicted maps of rabbit density and abundance show high levels of interannual variation
403 along the east coast of Australia, with density classes and abundances fluctuating between

404 high and low levels inland from the coast for a distance of ~300km (Figure 3). Hindcasts of
405 abundance for the southern coastline of mainland Australia showed lower inter-annual
406 variability compared to the eastern coastline. Inland areas tended to be relatively stable,
407 however, these areas were generally inside the low-confidence mask.

408 Analysis of temporal hotspot conditions suggest small inter-annual variability in the
409 threshold used to identify hotspots of rabbit abundance across time (mean = 12, S.D. = 2.5;
410 Figure 6). A Mann-Kendall trend test suggested a very small but non-significant increase in
411 the hotspot threshold across all years ($\tau = 0.05$, $p = 0.70$) suggesting rabbit numbers are
412 decreasing as the threshold used to identify a hotspot has increased. Broadly, hotspots of
413 rabbit abundance followed similar patterns to maps of predicted abundance (Figure 6). All
414 hotspot maps are provided in Data S1: Brown_et_al_RabbitAnalysisOutputs.nc, with code to
415 reproduce the analysis and Figure 6 provided in Data S1: RabbitHotspotAnalysis.R.

416 **Discussion:**

417 We show that combining multi-level hierarchical Bayesian models with simple machine
418 learning methods is an effective, and computationally tractable, method for modelling the
419 structure and dynamics of the geographical distribution of a wide-ranging invasive vertebrate
420 species. By allowing us to project, effectively, spatiotemporal variation in the abundance of
421 rabbit populations across their invasive range in Australia, our approach provides an
422 important new approach for identifying hotspots of persistently high rabbit abundance at
423 timescales (annual to decadal) that are directly relevant to resource management in Australia
424 (Hobday et al. 2010, Cooke 2012). The identification of potential past and future hotspots
425 will allow pest managers to better plan for and conduct control actions for rabbits in areas and
426 at times of greatest need (Simberloff 2003).

427 A robust understanding of spatiotemporal variability in abundance patterns across an
428 invasive species range is invaluable for studying the processes of invasion and for pest
429 management (Strayer et al. 2006). However, this requires spatial abundance estimates that
430 account for inherent biases in long-term count data (Joseph et al. 2009, Link et al. 2018). Our
431 use of a hierarchical Bayesian N-mixture model, coupled with a hyperprior-based model,

432 allowed us to explicitly account for important variation in detection probability in long-term
433 estimates of abundance from sites covering a large spatiotemporal extent. Although similar
434 approaches have been applied to rabbit spotlight count data before (Aubry et al. 2012, Wells
435 et al. 2016b), they have not then been extended to account for seasonal bias in counts from
436 multiple surveys at multiple sites, and have not been used to for predictions of spatiotemporal
437 abundance. Daily precipitation has previously been found to drastically decrease surface
438 activity of rabbits and therefore detectability (Ballinger and Morgan 2002), whilst the results
439 of our analysis suggest very small increases in detectability with increased rainfall on the day
440 of the survey. We found that increases in daily maximum temperature could either increase or
441 decrease the probability of detection across climate zones – this variability could be attributed
442 to differences in climate, or differences in survey time. For example, in climate zone 9
443 (warm, semi-arid conditions; Appendix S1: Table S2) increases in maximum daily
444 temperature increased detection probability, but if these surveys were mainly conducted in
445 the Austral winter (June, July, August) then maximum daily temperatures would be lower
446 than in, for example, climate zone 8 (warm, summer rainfall; Appendix S1: Table S2) (where
447 increases in maximum temperature decreased detection probability) if surveys in that zone
448 were mainly conducted in the Austral summer (DJF). Time of day and year has been shown
449 to influence counts during spotlight surveys (Ballinger and Morgan 2002, Williams et al.
450 2007, Barrio et al. 2009), with seasonal variations in Mediterranean environments also
451 reported (Martins et al. 2003). These variations have largely been attributed to changes in
452 foraging activities and seasonal variations in population abundances. Whilst information on
453 spotlight survey time (dawn, dusk, hour etc.) is missing from the database, we attempted to
454 overcome seasonal variability by using random regression models (Wilson et al. 2005) which
455 accounted for the month of survey mainly to control for seasonal birth pulsing (Wells et al.
456 2016b).

457 Our Bayesian hierarchical N-mixture model, employed at multiple sites across the
458 invasive range of rabbits in Australia, generated a standardized relative yearly rabbit
459 abundance across space and time, corrected for ‘false variation’ as a result of imperfect
460 detection and seasonal fluctuations in abundance (due to seasonal birth pulses) in some areas.

461 Using these corrected abundances in a machine learning framework (random forest models;
462 RF) provided a highly computationally efficient method for identifying the spatiotemporal
463 drivers of heterogeneity in rabbit abundance across their invasive range. Furthermore, the use
464 of RF permitted the analysis of non-linear relationships between, and within, predictor
465 variables, that may have otherwise been missed (Breiman 2001, Apley 2016).

466 The comprehensive nature of the statistical modelling undertaken here, covering 41
467 years and approximately 3.8 million square kilometers, which is unique for a terrestrial
468 invasive vertebrate, allowed us to directly model potential drivers of rabbit abundance in
469 space and time. Our results support previous research, showing that rabbit populations are
470 influenced by pasture availability and the water content of pastures (Cooke 2012),
471 temperature (attaining higher densities in cooler temperatures; Gilbert et al. 1987) and to an
472 extent, the effects of RCV-A1 (Cooke et al. 2018b). The effects of pasture availability and
473 water content (e.g. the presence of irrigated pastures), combined with cooler temperatures and
474 stable seasonal rainfall could potentially be driving the high predicted densities inland along
475 the southern coastline (Figure 3). The classification RF shows that RCV-A1 prevalence was
476 positively correlated with high rabbit densities (high/low), because RCV-A1 provides partial
477 protection from lethal RHDV (Strive et al. 2013). Since the prevalence of RCV-A1 is
478 strongly correlated with rainfall (Liu et al. 2014), rabbits in cooler, wetter areas are likely to
479 be found in higher abundances due to food availability, and these same populations are likely
480 to be more resistant to infection with lethal RHDV. Although, RCV-A1 also influenced
481 estimates of abundance from the regression RF, prevalence of RCV-A1 was negatively
482 associated with rabbit abundance – a result likely due to complex interactions between rabbit
483 populations, climatic conditions, disease vectors, and epizootics (Cooke 1983, Liu et al.
484 2014). This result requires further investigation, using new approaches that can directly tease
485 apart these interactions, which are often mutually reinforcing (Wells et al. 2018). The
486 presence of European rabbit fleas was not important in determining either density or
487 abundance, but has been shown previously to decrease rabbit numbers as a vector of the
488 myxoma virus (Cooke 1983). These results are likely a result of a lack of spatial and

489 temporally explicit data on the release, establishment and expansion of European fleas over
490 the study period.

491 Spatial and temporally explicit estimations of abundance are an important component
492 in ecological modelling, because a change in population abundance over time and space is
493 brought about by changes in movement and/or birth and death rates. Identifying and
494 quantifying the temporal variability in populations of invasive species can help to better
495 target management actions (Simberloff 2003) – particularly when responses to removal of
496 invasive species happen on varying time scales (Strayer et al. 2006, Cooke 2012, Lurgi et al.
497 2018), and different control measures will have differing population level effects (Wells et al.
498 2016a). Just as importantly, quantifying variability in population abundances across the range
499 of a species can unlock the ecological mechanisms responsible for spatiotemporal variation in
500 abundance across a species geographic distribution (Caughley et al. 1988). This information
501 is essential for optimizing management actions aimed at controlling invasive species (Mellin
502 et al. 2016). The clustered nature of the spotlight survey data (Figure 2; Roy-Dufresne et al.
503 2019a) resulted in large areas of our predicted density and abundance values falling inside
504 our low confidence mask (Figure 3). However, we still have faith in the predicted values at
505 these sites due to the results of our random forest models, and the climatic mask that was
506 used to prevent any extrapolation in our predictions. Due to the highly fluctuating nature of
507 rabbit populations, we believe that managers should still utilize such information to guide
508 potential future monitoring and management activities. The results also demonstrate that
509 despite using the most extensive dataset available, accurate spatio-temporal predictions of
510 population density and abundance of highly fluctuating species is an ongoing challenge.

511 The concept of a hotspot is focused on the stability of a species population, or a
512 measure of biodiversity, across space and over time (Mittermeier et al. 2011). Since
513 identifying priority areas for control activities is a key component in managing invasive
514 species (Lurgi et al. 2016), our hindcasts of areas where a higher than expected number of
515 rabbits can be found historically (hotspots), reveal priority sites for rabbit management.
516 Efforts towards eradication and control of rabbits in areas that are consistently identified as
517 hotspots (i.e. high proportion of time as a hotspot) should be given top priority (Lurgi et al.

518 2016), and rabbits of all age classes should be targeted (Wells et al. 2016a). Near-term
519 climate forecasts from regional climate models are now readily available at the temporal and
520 spatial resolutions needed to effectively manage biodiversity in response to global change
521 (Tabor and Williams 2010). Integrating these forecasts into our hotspot analysis would allow
522 areas for future rabbit management to be prioritized, based on knowledge of what the
523 abundance pattern is projected to be given forecast climate conditions, with the caveat that
524 inter-warren population competition and structure can occur at finer spatial resolutions than
525 the 5km² spatial scale used in this study (Lurgi et al. 2016). A comparable approach is
526 commonly used in fisheries management to set catch rates in space and time, with good
527 success (Hobday et al. 2010). Furthermore, these same spatiotemporal estimates of density
528 and abundance can be integrated into spatially explicit models for informing pest
529 management (Mellin et al. 2016), examining multispecies interactions (Lurgi et al. 2018), or
530 for inferring patterns of spatial variation in demographic rates (Hone 1999).

531 Beyond rabbits, our method of detecting hotspots could be used to strengthen theory
532 underpinning important concepts in invasion biology, including whether species' populations
533 with high but variable abundance are more sensitive to control interventions than populations
534 with high and less variable abundances (Wells et al. 2016a). The hypothesis being, that
535 populations that are consistent hotspots of abundance, are likely to be more resilient to
536 environmental fluctuations and, therefore, better able to recover from management
537 interventions if not completely eradicated (Mutze et al. 2010). Likewise, the method could be
538 used to test whether hotspots of abundance tend to occur more frequently at the center of the
539 range of an invasive species, as would be expected, based on theory (i.e., species abundance
540 distribution; Lawton 1993)

541 The spotlight count data in the Australian National Rabbit Database includes some
542 studies set up to record trends in rabbit population abundances after active (e.g. warren
543 ripping) or passive (e.g., release of RHDV) population control. The timing and extent of these
544 management actions are not extensively documented, potentially biasing abundance records
545 used in this analysis. While we tried to account for this variation by using data source as a
546 detectability covariate, the absence of detailed information on type and timing of

547 management intervention prevented a more thorough analysis of this potential source of
548 uncertainty. This bias could possibly have resulted in lower frequencies of high abundance
549 records for some areas, and therefore it is possible that some sites were not correctly
550 identified as hotspots in years directly following management intervention. However, our
551 CRFD hotspot thresholds are well below those shown to influence vegetation community
552 composition (Mutze et al. 2016), and as such any identified hotspots are still valuable for
553 management as these areas would still be identified as priority control sites at abundances
554 lower than those known to alter, for example, vegetation communities.

555 Our modelling approach for rabbits is applicable to any species for which long-term
556 spatially explicit monitoring data and high temporal resolution climate data are available. It is
557 flexible with regards to spatial grain and extent, and benefits from the utilization of
558 computationally efficient machine learning methods for generating maps of spatial
559 abundance, and for estimating variable interactions that link patterns of abundances to
560 potential drivers and processes. The long-term management of invasive species relies on
561 informed future projections of abundance and a good understanding of the processes that
562 underpin the structure and dynamics of a species past and present-day distribution in its
563 invasive range. Model-based approaches such as those created in this study promise to help
564 guide adaptive management approaches by permitting inferences to be made regarding likely
565 future population trends at scales relevant to management.

566 **Acknowledgements:**

567 This research was funded by an Australian Research Council (ARC) Linkage Project
568 (LP12020024) and Future Fellowship (FT140101192). We would like to thank Greg Mutze
569 for discussions and advice regarding preliminary analysis and outputs.

570 **Literature cited:**

571 Apley, D. W. 2016. Visualizing the effects of predictor variables in black box supervised
572 learning models. arXiv preprint arXiv:1612.08468.
573 Aubry, P., D. Pontier, J. Aubineau, F. Berger, Y. Léonard, B. Mauvy, and S. Marchandeanu.
574 2012. Monitoring population size of mammals using a spotlight-count-based

575 abundance index: How to relate the number of counts to the precision? Ecological
576 indicators **18**:599-607, doi:10.1016/j.ecolind.2012.01.019.

577 Baker, C. M., and M. Bode. 2016. Placing invasive species management in a spatiotemporal
578 context. Ecological Applications **26**:712-725, doi:10.1890/15-0095.

579 Ballinger, A., and D. G. Morgan. 2002. Validating two methods for monitoring population
580 size of the European rabbit (*Oryctolagus cuniculus*). Wildlife Research **29**:431-437,
581 doi:10.1071/wr01055.

582 Barrio, I. C., P. Acevedo, and F. S. Tortosa. 2009. Assessment of methods for estimating wild
583 rabbit population abundance in agricultural landscapes. European Journal of Wildlife
584 Research **56**:335-340, doi:10.1007/s10344-009-0327-7.

585 Bartolino, V., L. Maiorano, and F. Colloca. 2011a. A frequency distribution approach to
586 hotspot identification. Population Ecology **53**:351-359, doi:10.1007/s10144-010-
587 0229-2.

588 Bartolino, V., L. Maiorano, and F. Colloca. 2011b. Frequency distribution curves and the
589 identification of hotspots: response to comments. Population Ecology **53**:603-604,
590 doi:10.1007/s10144-011-0273-6.

591 Breiman, L. 2001. Random forests. Machine learning **45**:5-32,
592 doi:10.1023/a:1010933404324.

593 Buckland, S. T., E. A. Rexstad, T. A. Marques, and C. S. Oedekoven. 2015. Distance
594 sampling: methods and applications. Springer, Heidelberg.

595 Cabral, J. S., and F. M. Schurr. 2010. Estimating demographic models for the range dynamics
596 of plant species. Global Ecology and Biogeography **19**:85-97, doi:10.1111/j.1466-
597 8238.2009.00492.x.

598 Caughley, G., D. Grice, R. Barker, and B. Brown. 1988. The edge of the range. Journal of
599 Animal Ecology **57**:771-785, doi:10.2307/5092.

600 Cayuela, L., L. Gálvez-Bravo, L. M. Carrascal, and F. S. de Albuquerque. 2011. Comments
601 on Bartolino et al. (2011): limits of cumulative relative frequency distribution curves
602 for hotspot identification. Population Ecology **53**:597, doi:10.1007/s10144-011-0272-
603 7.

604 Channell, R., and M. V. Lomolino. 2000. Dynamic biogeography and conservation of
605 endangered species. *Nature* **403**:84-86, doi:10.1038/47487.

606 Cooke, B. 1983. Changes in the Age-Structure and Size of Populations of Wild Rabbits in
607 South Australia, Following the Introduction of European Rabbit Fleas, *Spilopsyllus*
608 *cuniculi* (Dale), as Vectors of Myxomatosis. *Wildlife Research* **10**:105-120,
609 doi:10.1071/WR9830105.

610 Cooke, B. 2012. Rabbits: manageable environmental pests or participants in new Australian
611 ecosystems? *Wildlife Research* **39**:279-289, doi:10.1071/WR11166.

612 Cooke, B., M. Brennan, and P. Elsworth. 2018a. Ability of wild rabbit, *Oryctolagus*
613 *cuniculus*, to lactate successfully in hot environments explains continued spread in
614 Australia. *Wildlife Research* **45**:267-273, doi:10.1071/wr17177.

615 Cooke, B., P. Chudleigh, S. Simpson, and G. Saunders. 2013. The Economic Benefits of the
616 Biological Control of Rabbits in Australia, 1950–2011. *Australian Economic History*
617 *Review* **53**:91-107, doi:10.1111/aehr.12000.

618 Cooke, B., R. P. Duncan, I. McDonald, J. Liu, L. Capucci, G. J. Mutze, and T. Strive. 2018b.
619 Prior exposure to non-pathogenic calicivirus RCV-A1 reduces both infection rate and
620 mortality from rabbit haemorrhagic disease in a population of wild rabbits in
621 Australia. *Transboundary and Emerging Diseases* **65**:e470-e477,
622 doi:10.1111/tbed.12786.

623 Cooke, B. D. 1977. Factors limiting the distribution of the wild rabbit in Australia.
624 *Proceedings of the Ecological Society of Australia* **10**:113-120.

625 Cox, G. W. 2013. *Alien Species and Evolution: The Evolutionary Ecology of Exotic Plants,*
626 *Animals, Microbes, and Interacting Native Species.* Island Press, Washington.

627 Delibes-Mateos, M., M. Delibes, P. Ferreras, and R. Villafuerte. 2008. Key role of European
628 rabbits in the conservation of the Western Mediterranean basin hotspot. *Conservation*
629 *Biology* **22**:1106-1117, doi:10.1111/j.1523-1739.2008.00993.x.

630 Elith, J., M. Kearney, and S. Phillips. 2010. The art of modelling range-shifting species.
631 *Methods in Ecology and Evolution* **1**:330-342, doi:10.1111/j.2041-
632 210X.2010.00036.x.

633 Fordham, D., H. Akçakaya, M. Araújo, B. Brook, J. Brodie, E. Post, and D. Doak. 2012.
634 Modelling range shifts for invasive vertebrates in response to climate change. *in*
635 Brodie J, Post E, and D. D, editors. *Wildlife Conservation in a Changing Climate*.
636 University of Chicago Press, Chicago.

637 Fordham, D., H. R. Akcakaya, M. B. Araujo, D. A. Keith, and B. W. Brook. 2013a. Tools for
638 integrating range change, extinction risk and climate change information into
639 conservation management. *Ecography* **36**:956-964, doi:10.1111/j.1600-
640 0587.2013.00147.x.

641 Fordham, D., H. R. Akçakaya, B. W. Brook, A. Rodríguez, P. C. Alves, E. Civantos, M.
642 Triviño, M. J. Watts, and M. B. Araújo. 2013b. Adapted conservation measures are
643 required to save the Iberian lynx in a changing climate. *Nature Climate Change* **3**:899,
644 doi:10.1038/nclimate1954.

645 Gaston, K. J. 2003. *The structure and dynamics of geographic ranges*. Oxford University
646 Press, New York.

647 Gelman, A., X. L. Meng, and H. Stern. 1996. Posterior predictive assessment of model fitness
648 via realized discrepancies. *Statistica sinica* **6**:733-760.

649 Gilbert, N., K. Myers, B. D. Cooke, J. D. Dunsmore, P. J. Fullagar, J. A. Gibb, D. R. King, I.
650 Parer, S. H. Wheeler, and D. H. Wood. 1987. Comparative Dynamics of Australasian
651 Rabbit-Populations. *Wildlife Research* **14**:491-503, doi:10.1071/wr9870491.

652 Guillera-Aroita, G. 2017. Modelling of species distributions, range dynamics and
653 communities under imperfect detection: advances, challenges and opportunities.
654 *Ecography* **40**:281-295, doi:10.1111/ecog.02445.

655 Hobday, A. J., J. R. Hartog, T. Timmiss, and J. Fielding. 2010. Dynamic spatial zoning to
656 manage southern bluefin tuna (*Thunnus maccoyii*) capture in a multi-species longline
657 fishery. *Fisheries Oceanography* **19**:243-253, doi:10.1111/j.1365-2419.2010.00540.x.

658 Hone, J. 1999. On rate of increase (r): patterns of variation in Australian mammals and the
659 implications for wildlife management. *Journal of Applied Ecology* **36**:709-718,
660 doi:10.1046/j.1365-2664.1999.00439.x.

661 Hosmer, D. W., S. Lemeshow, and R. X. Sturdivant. 2013. Applied Logistic Regression. 3rd
662 edition. John Wiley & Sons, Hoboken, NJ, USA.

663 Joseph, L. N., C. Elkin, T. G. Martin, and H. P. Possingham. 2009. Modeling abundance
664 using N-mixture models: the importance of considering ecological mechanisms.
665 *Ecological Applications* **19**:631-642, doi:10.1890/07-2107.1.

666 Kéry, M., and M. Schaub. 2011. Bayesian Population Analysis using WinBUGS: A
667 Hierarchical Perspective. Academic Press, Oxford.

668 Kuhn, M. 2018. caret: Classification and Regression Training.

669 Lawton, J. H. 1993. Range, population abundance and conservation. *Trends in Ecology &*
670 *Evolution* **8**:409-413, doi:10.1016/0169-5347(93)90043-O.

671 Liaw, A., and M. Wiener. 2018. Classification and Regression by randomForest.

672 Link, W. A., M. R. Schofield, R. J. Barker, and J. R. Sauer. 2018. On the robustness of N-
673 mixture models. *Ecology* **99**:1547-1551, doi:10.1002/ecy.2362.

674 Liu, J., D. A. Fordham, B. D. Cooke, T. Cox, G. Mutze, and T. Strive. 2014. Distribution and
675 prevalence of the Australian non-pathogenic rabbit calicivirus is correlated with
676 rainfall and temperature. *PLOS ONE* **9**:e113976, doi:10.1371/journal.pone.0113976.

677 Lurgi, M., E. G. Ritchie, and D. A. Fordham. 2018. Eradicating abundant invasive prey could
678 cause unexpected and varied biodiversity outcomes: The importance of multispecies
679 interactions. *Journal of Applied Ecology* **55**:2396-2407, doi:10.1111/1365-
680 2664.13188.

681 Lurgi, M., K. Wells, M. Kennedy, S. Campbell, and D. A. Fordham. 2016. A Landscape
682 Approach to Invasive Species Management. *PLOS ONE* **11**:e0160417,
683 doi:10.1371/journal.pone.0160417.

684 Magurran, A. E. 2007. Species abundance distributions over time. *Ecology letters* **10**:347-
685 354, doi:10.1111/j.1461-0248.2007.01024.x.

686 Magurran, A. E., S. R. Baillie, S. T. Buckland, J. M. Dick, D. A. Elston, E. M. Scott, R. I.
687 Smith, P. J. Somerfield, and A. D. Watt. 2010. Long-term datasets in biodiversity
688 research and monitoring: assessing change in ecological communities through time.
689 *Trends in Ecology & Evolution* **25**:574-582, doi:10.1016/j.tree.2010.06.016.

690 Martin, T. G., B. A. Wintle, J. R. Rhodes, P. M. Kuhnert, S. A. Field, S. J. Low-Choy, A. J.
691 Tyre, and H. P. Possingham. 2005. Zero tolerance ecology: improving ecological
692 inference by modelling the source of zero observations. *Ecology letters* **8**:1235-1246,
693 doi:10.1111/j.1461-0248.2005.00826.x.

694 Martins, H., H. Barbosa, M. Hodgson, R. Borralho, and F. Rego. 2003. Effect of vegetation
695 type and environmental factors on European wild rabbit (*Oryctolagus cuniculus*)
696 counts in a southern Portuguese montado. *Acta Theriologica* **48**:385-398,
697 doi:10.1007/bf03194177.

698 Mellin, C., M. Lurgi, S. Matthews, M. A. MacNeil, M. J. Caley, N. Bax, R. Przeslawski, and
699 D. A. Fordham. 2016. Forecasting marine invasions under climate change: Biotic
700 interactions and demographic processes matter. *Biological Conservation* **204**:459-467,
701 doi:10.1016/j.biocon.2016.11.008.

702 Mellin, C., B. D. Russell, S. D. Connell, B. W. Brook, and D. A. Fordham. 2012. Geographic
703 range determinants of two commercially important marine molluscs. *Diversity and*
704 *Distributions* **18**:133-146, doi:10.1111/j.1472-4642.2011.00822.x.

705 Mittermeier, R. A., W. R. Turner, F. W. Larsen, T. M. Brooks, and C. Gascon. 2011. Global
706 Biodiversity Conservation: The Critical Role of Hotspots. Pages 3-22 in F. E. Zachos
707 and J. C. Habel, editors. *Biodiversity Hotspots: Distribution and Protection of*
708 *Conservation Priority Areas*. Springer Berlin.

709 Mutze, G., P. Bird, J. Kovaliski, D. Peacock, S. Jennings, and B. Cooke. 2002. Emerging
710 epidemiological patterns in rabbit haemorrhagic disease, its interaction with
711 myxomatosis, and their effects on rabbit populations in South Australia. *Wildlife*
712 *Research* **29**:577-590, doi:10.1071/wr00100.

713 Mutze, G., B. Cooke, and S. Jennings. 2016. Estimating density-dependent impacts of
714 European rabbits on Australian tree and shrub populations. *Australian Journal of*
715 *Botany* **64**:142-152, doi:10.1071/bt15208.

716 Mutze, G., J. Kovaliski, K. Butler, L. Capucci, and S. McPhee. 2010. The effect of rabbit
717 population control programmes on the impact of rabbit haemorrhagic disease in

718 south-eastern Australia. *Journal of Applied Ecology* **47**:1137-1146,
719 doi:10.1111/j.1365-2664.2010.01844.x.

720 Noble, I. R. 1977. Long-Term Biomass Dynamics in an Arid Chenopod Shrub Community at
721 Koonamore, South Australia. *Australian Journal of Botany* **25**:639-653,
722 doi:10.1071/Bt9770639.

723 Pagel, J., B. J. Anderson, R. B. O'Hara, W. Cramer, R. Fox, F. Jeltsch, D. B. Roy, C. D.
724 Thomas, F. M. Schurr, and S. McMahon. 2014. Quantifying range-wide variation in
725 population trends from local abundance surveys and widespread opportunistic
726 occurrence records. *Methods in Ecology and Evolution* **5**:751-760, doi:10.1111/2041-
727 210x.12221.

728 Pech, R. P., and G. M. Hood. 1998. Foxes, rabbits, alternative prey and rabbit calicivirus
729 disease: consequences of a new biological control agent for an outbreaking species in
730 Australia. *Journal of Applied Ecology* **35**:434-453, doi:10.1046/j.1365-
731 2664.1998.00318.x.

732 Phillips, B. L., G. P. Brown, J. K. Webb, and R. Shine. 2006. Invasion and the evolution of
733 speed in toads. *Nature* **439**:803, doi:10.1038/439803a.

734 Plummer, M. 2016. rjags: Bayesian Graphical Models using MCMC.

735 Poole, W. E. 1960. Breeding of the of wild rabbit, *Oryctolagus cuniculus* (L.), in relation to
736 the environment. *CSIRO Wildlife Research* **5**:21-43.

737 R Core Team. 2017. R: A language and environment for statistical computing. R Foundation
738 for Statistical Computing, Vienna, Austria.

739 Rout, T. M., and T. Walshe. 2013. Accounting for Time Preference in Management
740 Decisions: An Application to Invasive Species. *Journal of Multi-Criteria Decision*
741 *Analysis* **20**:197-211, doi:10.1002/mcda.1490.

742 Roy-Dufresne, E., M. Lurgi, S. C. Brown, K. Wells, B. Cooke, G. Mutze, D. Peacock, P.
743 Cassey, D. Berman, B. W. Brook, S. Campbell, T. Cox, J. Daly, I. Dunk, P. Elsworth,
744 D. Fletcher, D. M. Forsyth, G. Hocking, J. Kovaliski, M. Leane, B. Low, M.
745 Kennedy, J. Matthews, S. McPhee, C. Mellin, T. Mooney, K. Moseby, J. Read, B. J.
746 Richardson, K. Schneider, E. Schwarz, R. Sinclair, T. Strive, F. Triulcio, P. West, F.

747 Saltre, and D. A. Fordham. 2019a. The Australian National Rabbit Database: 50 yr of
748 population monitoring of an invasive species. *Ecology* **100**:e02750,
749 doi:10.1002/ecy.2750.

750 Roy-Dufresne, E., F. Saltré, B. D. Cooke, C. Mellin, G. Mutze, T. Cox, and D. A. Fordham.
751 2019b. Modeling the distribution of a wide-ranging invasive species using the
752 sampling efforts of expert and citizen scientists. *Ecology and Evolution* **9**:11053-
753 11063, doi:10.1002/ece3.5609.

754 Royle, J. A. 2004. N-mixture models for estimating population size from spatially replicated
755 counts. *Biometrics* **60**:108-115, doi:10.1111/j.0006-341X.2004.00142.x.

756 Schurr, F. M., J. Pagel, J. S. Cabral, J. Groeneveld, O. Bykova, R. B. O'Hara, F. Hartig, W.
757 D. Kissling, H. P. Linder, G. F. Midgley, B. Schröder, A. Singer, and N. E.
758 Zimmermann. 2012. How to understand species' niches and range dynamics: a
759 demographic research agenda for biogeography. *Journal of Biogeography* **39**:2146-
760 2162, doi:10.1111/j.1365-2699.2012.02737.x.

761 Simberloff, D. 2003. How Much Information on Population Biology Is Needed to Manage
762 Introduced Species? *Conservation Biology* **17**:83-92, doi:10.1046/j.1523-
763 1739.2003.02028.x.

764 Sofaer, H. R., C. S. Jarnevich, and I. S. Pearse. 2018. The relationship between invader
765 abundance and impact. *Ecosphere* **9**:e02415, doi:10.1002/ecs2.2415.

766 Stodart, E., and I. Parer. 1988. Colonisation of Australia by the rabbit *Oryctolagus cuniculus*
767 (L.). Canberra, CSIRO.

768 Strayer, D. L., V. T. Eviner, J. M. Jeschke, and M. L. Pace. 2006. Understanding the long-
769 term effects of species invasions. *Trends in Ecology & Evolution* **21**:645-651,
770 doi:10.1016/j.tree.2006.07.007.

771 Strive, T., P. Elsworth, J. Liu, J. D. Wright, J. Kovaliski, and L. Capucci. 2013. The non-
772 pathogenic Australian rabbit calicivirus RCV-A1 provides temporal and partial cross
773 protection to lethal Rabbit Haemorrhagic Disease Virus infection which is not
774 dependent on antibody titres. *Veterinary research* **44**:51-51, doi:10.1186/1297-9716-
775 44-51.

776 Tabor, K., and J. W. Williams. 2010. Globally downscaled climate projections for assessing
777 the conservation impacts of climate change. *Ecological Applications* **20**:554-565,
778 doi:10.1890/09-0173.1.

779 Wells, K., P. Cassey, R. G. Sinclair, G. J. Mutze, D. E. Peacock, R. C. Lacy, B. D. Cooke, R.
780 B. O'Hara, B. W. Brook, and D. A. Fordham. 2016a. Targeting season and age for
781 optimizing control of invasive rabbits. *Journal of Wildlife Management* **80**:990-999,
782 doi:10.1002/jwmg.21093.

783 Wells, K., D. A. Fordham, B. W. Brook, P. Cassey, T. Cox, R. B. O'Hara, and N. I.
784 Schwensow. 2018. Disentangling synergistic disease dynamics: Implications for the
785 viral biocontrol of rabbits. *Journal of Animal Ecology* **87**:1418-1428,
786 doi:10.1111/1365-2656.12871.

787 Wells, K., R. B. O'Hara, B. D. Cooke, G. J. Mutze, T. A. Prowse, and D. A. Fordham. 2016b.
788 Environmental effects and individual body condition drive seasonal fecundity of
789 rabbits: identifying acute and lagged processes. *Oecologia* **181**:853-864,
790 doi:10.1007/s00442-016-3617-2.

791 Whittaker, R. J., M. B. Araújo, P. Jepson, R. J. Ladle, J. E. M. Watson, and K. J. Willis.
792 2005. Conservation Biogeography: assessment and prospect. *Diversity and*
793 *Distributions* **11**:3-23, doi:10.1111/j.1366-9516.2005.00143.x.

794 Williams, D., P. Acevedo, C. Gortázar, M. A. Escudero, J. L. Labarta, J. Marco, and R.
795 Villafuerte. 2007. Hunting for answers: rabbit (*Oryctolagus cuniculus*) population
796 trends in northeastern Spain. *European Journal of Wildlife Research* **53**:19-28,
797 doi:10.1007/s10344-006-0056-0.

798 Wilson, A. J., L. E. Kruuk, and D. W. Coltman. 2005. Ontogenetic patterns in heritable
799 variation for body size: using random regression models in a wild ungulate
800 population. *American Naturalist* **166**:E177-192, doi:10.1086/497441.

801 Yoccoz, N. G., J. D. Nichols, and T. Boulinier. 2001. Monitoring of biological diversity in
802 space and time. *Trends in Ecology & Evolution* **16**:446-453, doi:10.1016/S0169-
803 5347(01)02205-4.

804

805 **Data Accessibility Statement:**

806 All output maps (netcdf format) and R code to reproduce the hotspot analysis and Figure 6 is
807 available in Data S1. Spotlight data used for the analysis is available in Roy-Dufresne et al.
808 (2019a).

809 **Tables:**

810 **Table 1:** Coefficient estimates (\pm S.D) for the climatic covariates used to model detection
 811 probability of rabbits during spotlight surveys in different climate zones. Geographic
 812 locations of the climate zones can be found in Figure 2. Descriptions of the climate zones are
 813 provided in Appendix S1: Table S2.

Climate Zone	Daily maximum temperature	Daily minimum temperature	Daily Precipitation
1	-0.02 (0.10)	0.08 (0.11)	0.05 (0.05)
2	-0.34 (0.15)	0.04 (0.11)	0.03 (0.05)
3	0.52 (0.17)	0.00 (0.11)	0.07 (0.13)
4	-0.30 (0.21)	-0.02 (0.14)	0.04 (0.12)
5	0.02 (0.41)	0.03 (0.17)	0.05 (0.14)
6	-0.28 (0.23)	0.00 (0.10)	0.05 (0.09)
7	-0.20 (0.17)	0.01 (0.13)	0.01 (0.10)
8	0.26 (0.17)	0.09 (0.12)	0.08 (0.11)
9	0.30 (0.13)	0.07 (0.10)	0.07 (0.09)

814 **Table 2:** Performance of the random forest regression and classification models. Cross validated model performance was assessed using 1000
815 repeats of Monte-Carlo cross validation with an 80/20 (train/test) split. Accuracy of both the regression and classification models was excellent
816 across climate zones and in most cases fair to excellent within climate zones (Hosmer et al. 2013). For climate zones 5 and 7, mean balanced
817 accuracy and true skill statistics could not be calculated as the classification model predicted all samples as belonging to the same class.

	Classification				Regression		
	Sensitivity	Specificity	Mean Balanced Accuracy	True Skill Statistic	Mean observed	Mean predicted	Mean absolute error
Overall	0.86	0.85	0.86	0.71	6.4 (\pm 11.9)	4.9 (\pm 6.4)	1.5
Climate Zone							
1	0.68	0.76	0.72	0.44	8.7 (\pm 13.9)	6.2 (\pm 6.6)	2.6
2	0.87	0.50	0.68	0.37	5.7 (\pm 9.9)	4 (\pm 5.8)	1.7
3	0.60	1.00	0.80	0.60	14.7 (\pm 20.1)	10 (\pm 8.2)	4.7
4	0.49	0.87	0.68	0.36	11.5 (\pm 16.3)	8.6 (\pm 6.4)	2.9
5	NA	1.00	NA	NA	7.4 (\pm 7.3)	6.2 (\pm 1.9)	1.2
6	0.67	0.90	0.78	0.57	5.3 (\pm 6.9)	5.2 (\pm 4.3)	0.1
7	1.00	NA	NA	NA	1.6 (\pm 2.5)	1.4 (\pm 1.1)	0.1
8	0.88	0.68	0.78	0.56	12.9 (\pm 15.4)	11 (\pm 11)	2.0
9	0.99	0.50	0.75	0.49	2.1 (\pm 4.1)	1.6 (\pm 1.4)	0.6

818 **Figure legends:**

819 Figure 1: The modelling approach used to correct records of abundance from spotlight
820 surveys and produce maps of rabbit density, abundance, and hotspots. The hierarchical
821 Bayesian N-Mixture model was created using abundance records from spotlight survey data
822 and covariates linked to detection probability (a). The bias-corrected outputs of this model
823 were then used to make spatiotemporal explicit predictions of rabbit density (b) and
824 abundance (c). Note that the random forest abundance estimation (c) was dependent on the
825 random forest density classification (b) as both a point based measure (i.e. for training the
826 abundance model), and as a continuous spatial coverage (i.e. for predicting maps of estimated
827 abundance). Items with a dashed outline represent point-based (i.e. individual grid-cell) data,
828 solid outlines represent continuous spatial coverage (i.e. pixels over the entire grid). Arrows
829 show the connections between the various elements.

830

831 Figure 2: Map showing the location of all spotlight rabbit abundance records (1971-2012)
832 and the sites used in the final analysis. Column plots show the relative magnitudes for
833 observed (dark grey) and Bayesian model corrected abundance (light grey) for a selection of
834 sites. The different colors represent the nine climatic zones that were used in our analysis.
835 Descriptions of the climate zones are in Appendix S1: Table S2. The beige color represents
836 areas that are outside of the climatic envelope of our sampling sites. Map is projected in GDA
837 1994 Australian Albers (EPSG:3577).

838

839 Figure 3: Spatial predictions of rabbit densities and abundances inferred from the random
840 forest models. (a) Spatial variation in the mode of predicted corrected densities between 1972
841 and 2012. (b) Mean corrected abundance (rabbits/km of transect) between 1973 and 2012. (c)
842 The probability of a correct model classification (low/high), with darker colors (dark
843 green/dark red) indicative of high confidence in the predicted class. (d) The standard
844 deviation of the predicted corrected abundances between 1973 and 2012. All maps are
845 masked to the climatic envelope of the climate zones shown in Figure 2. The muted colors

846 represent areas with low prediction confidence i.e., pixels where the model is forced to
847 extrapolate beyond the climate and environmental envelope used to calibrate the model.
848 Maps are projected in GDA 1994 Australian Albers (EPSG:3577).

849

850 Figure 4: Accumulated Local Effects (ALE) plots of four important variables depicting the
851 variation in rabbit abundance across environmental gradients. Values on the y-axes represent
852 changes in abundance from the average sample conditional on the values on the x-axes (a).
853 The rug plots on the inside of the x-axis show the distribution of sites across that variable.
854 The 3-dimensional plots (b, c) show the second-order effects of benign RCV-A1 calicivirus
855 with two climatic variables; average temperature two years prior to the survey (b), and total
856 precipitation the year prior to the survey (c), after removing the main effects of the features.
857 In other words, panels b and c only show the additional interaction effect of the two features.
858 The colors correspond to the values on the z-axis, with reds indicating a more positive effect
859 on abundances.

860

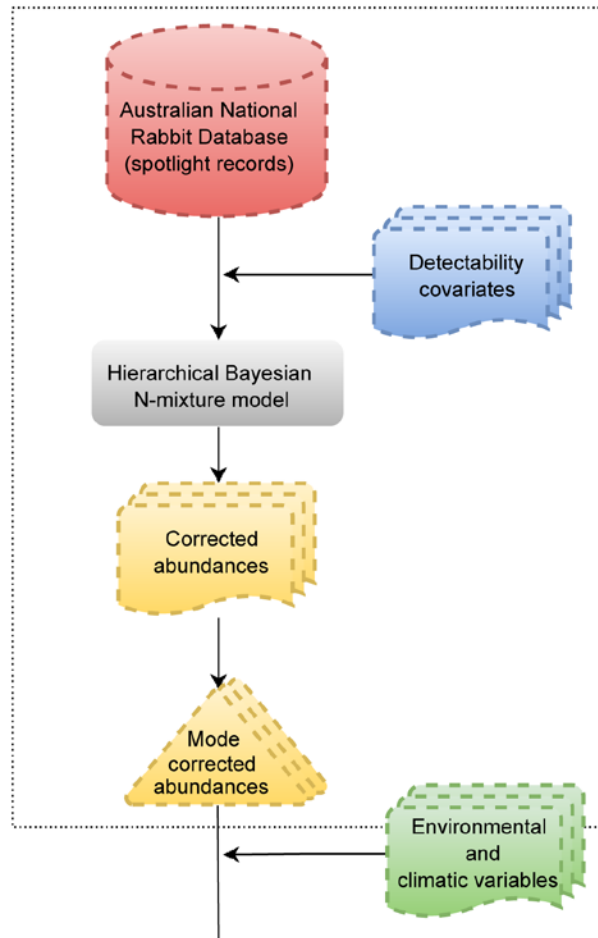
861 Figure 5: Empirically corrected abundance estimates (i.e. corrected; black line) and projected
862 (blue line) abundance estimates of rabbits for nine selected climate zones in Australia. Points
863 display the median estimates of corrected abundance estimates and predicted abundances
864 (based on the random forest regression model) across all sites within a climate zone for a
865 given year. The lines are for connecting points between sampling years, but do not represent
866 the estimates between years, and show the discontinuous nature of the sampling within some
867 climate zones. The blue bandings represent the 95% (light blue) and 50% (dark blue)
868 prediction intervals for the regression model predictions within each zone.

869

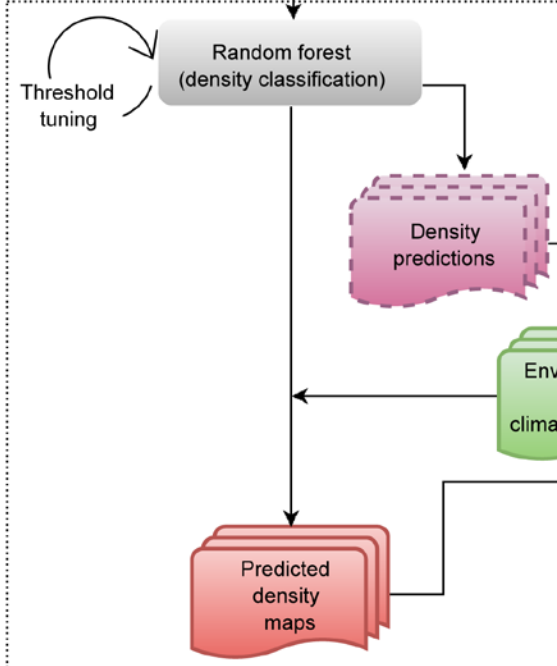
870 Figure 6: Percent time spent in hotspot conditions for high rabbit abundances. Values for
871 each cell (a) represent the proportion of time (between 1973 and 2012) that cells were
872 considered “hotspots” of rabbit abundance. The map is masked to the climatic envelope of
873 the climate zones shown in Figure 2. Muted colors represent areas with low prediction
874 confidence i.e., pixels where the RF model was forced to extrapolate beyond the climate and

875 environmental envelope used to calibrate the model. Map is projected in GDA 1994
876 Australian Albers (EPSG:3577). The cumulative relative distribution frequency plots (b)
877 show the inter-annual variability in rabbit populations for the RF predicted abundances that
878 were used to define hotspot thresholds.

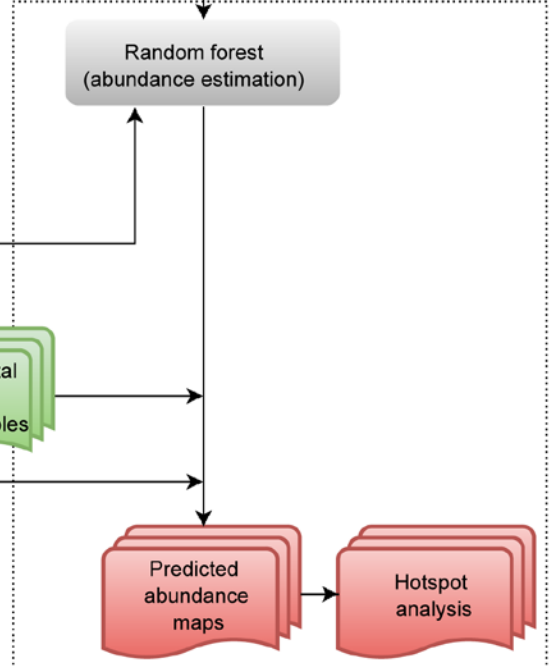
a



b

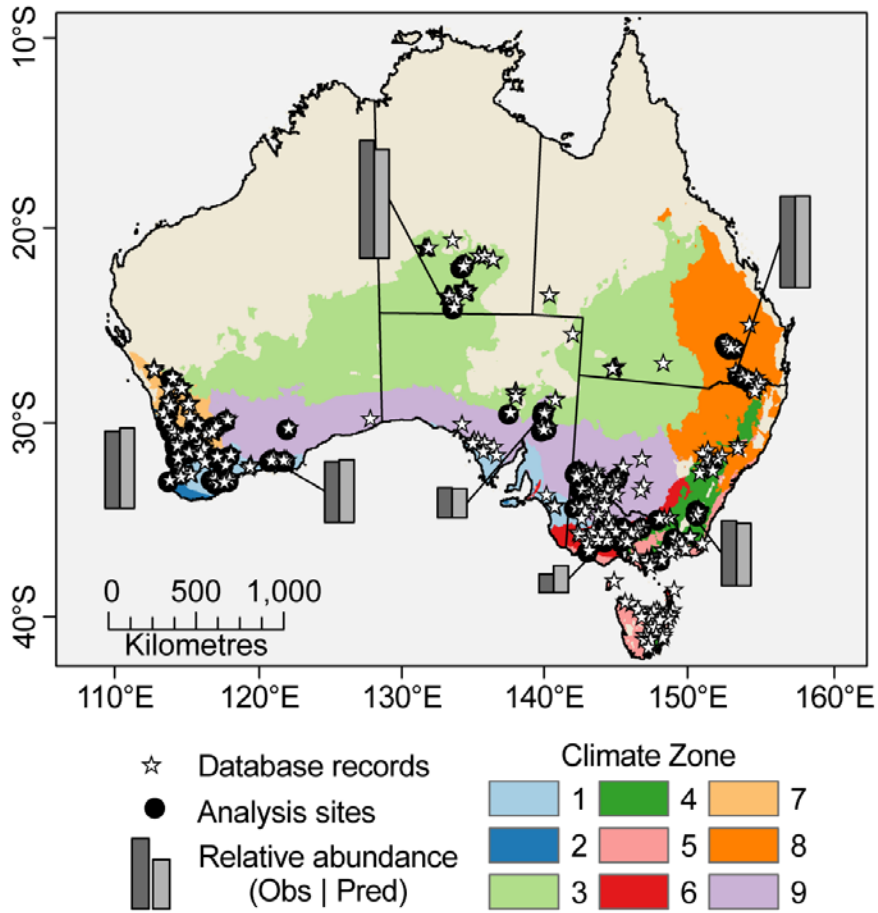


c



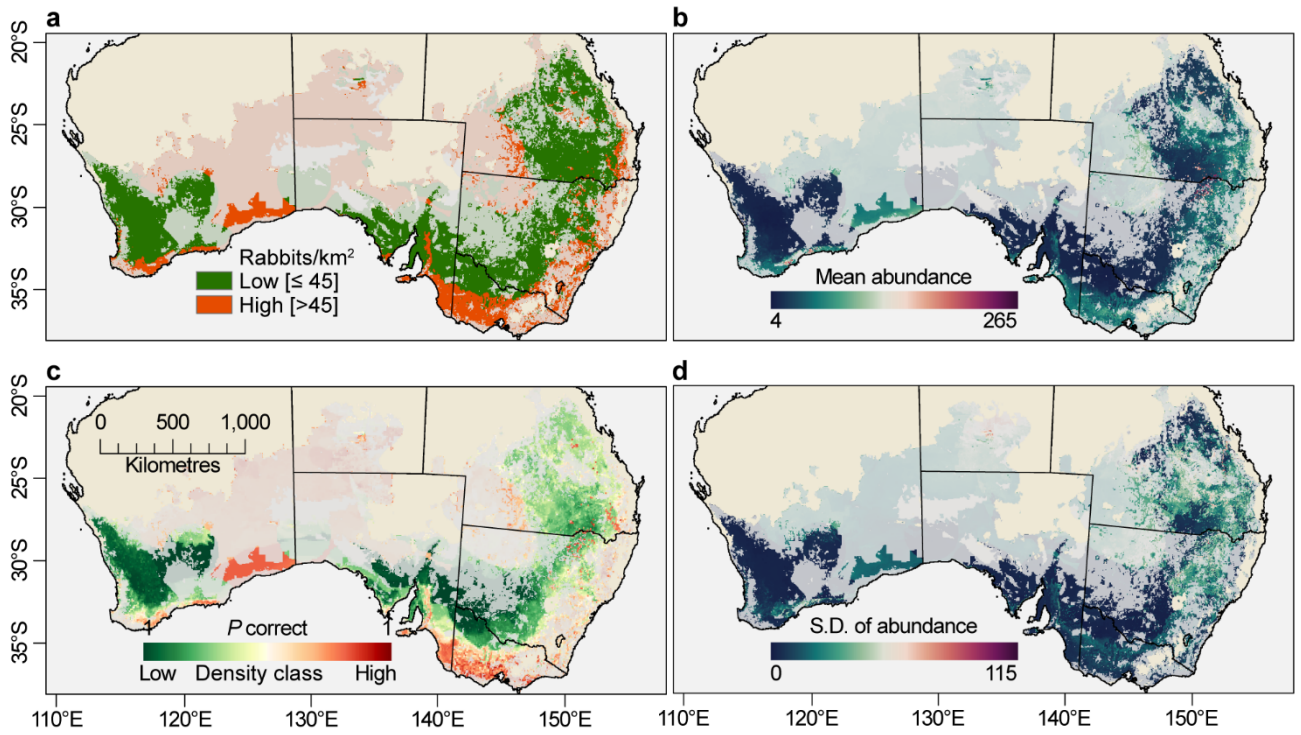
880

881 **Figure 1**



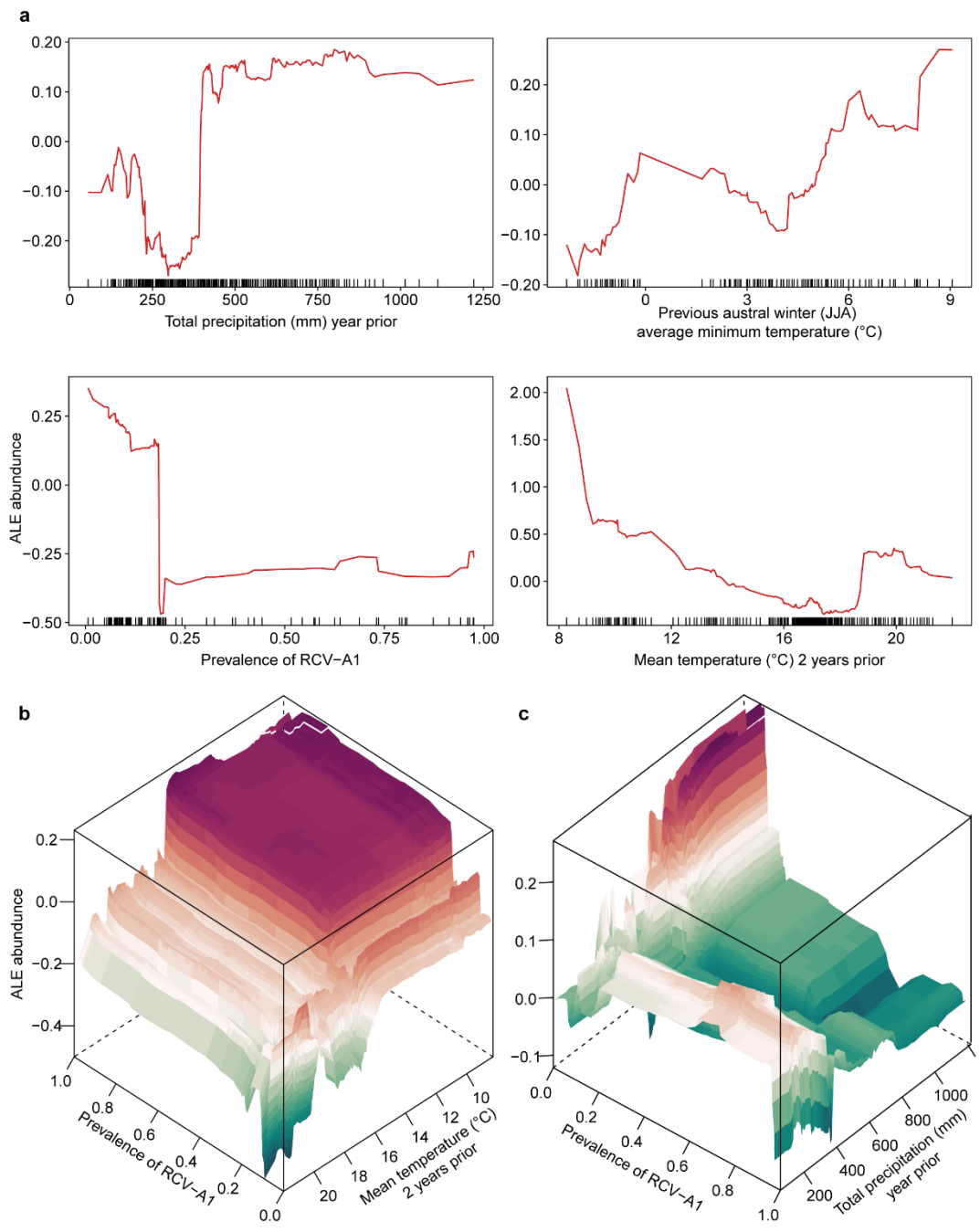
882

883 Figure 2



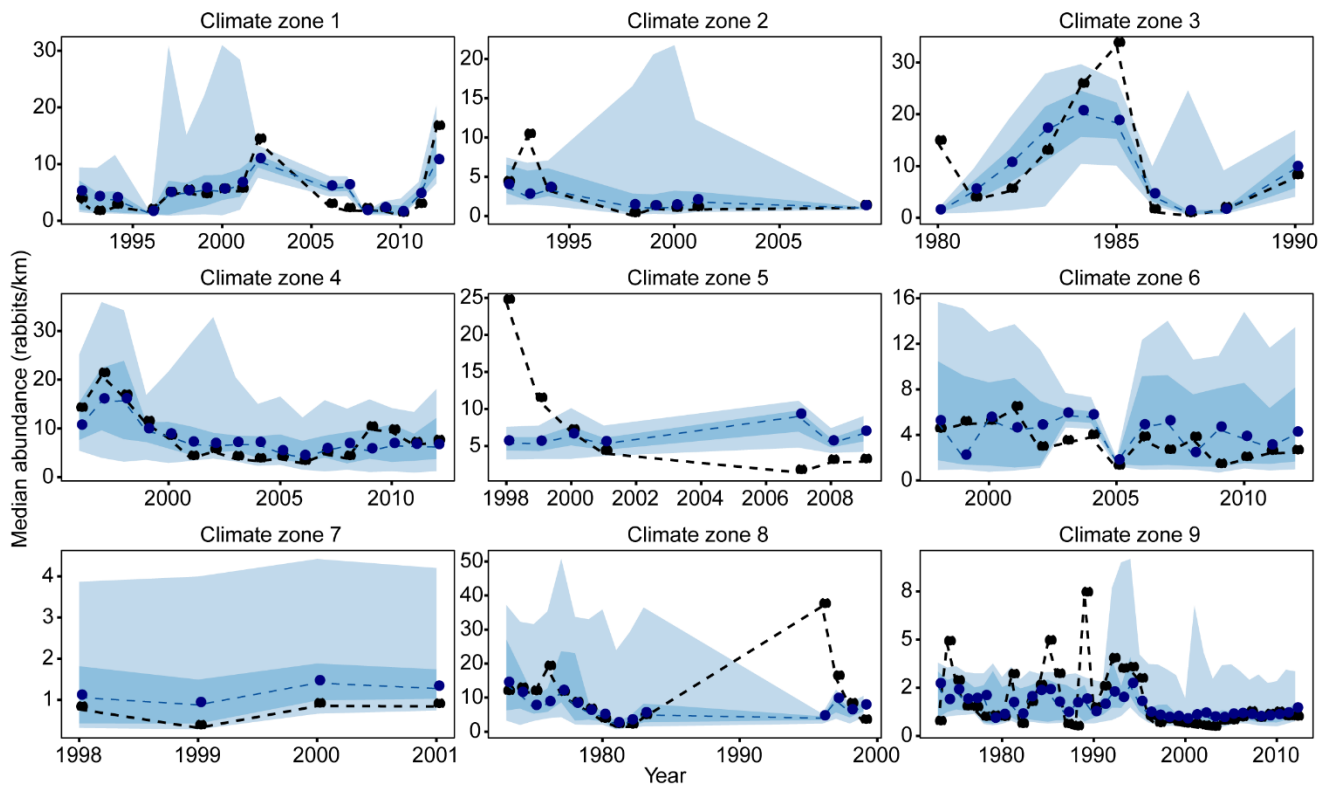
884

885 Figure 3



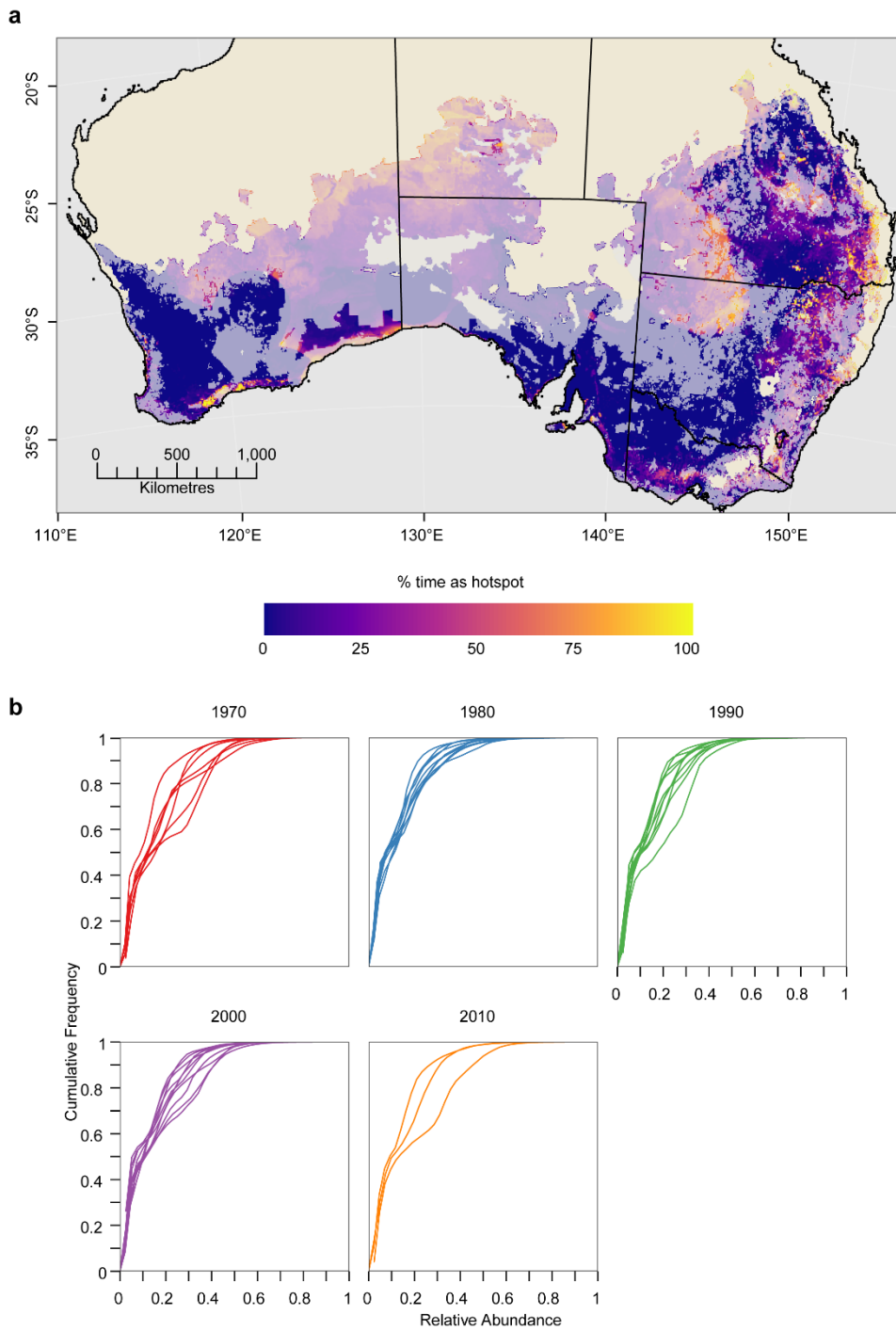
886

887 Figure 4



888

889 Figure 5



890

891 Figure 6